

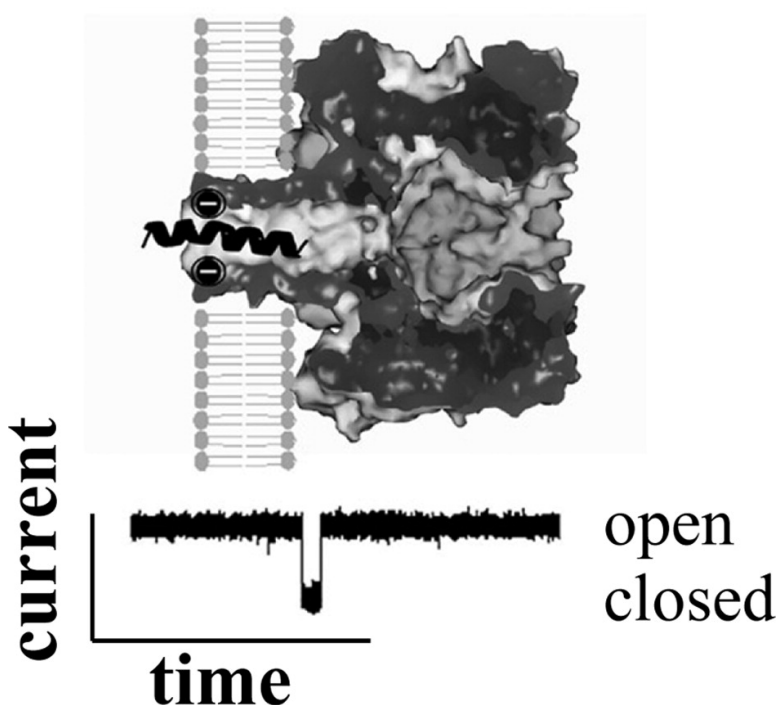
Article

## Catalyzing the Translocation of Polypeptides through Attractive Interactions

Aaron J. Wolfe, Mohammad, Stephen Cheley, Hagan Bayley, and Liviu Movileanu

*J. Am. Chem. Soc.*, **2007**, 129 (45), 14034-14041 • DOI: 10.1021/ja0749340 • Publication Date (Web): 19 October 2007

Downloaded from <http://pubs.acs.org> on February 14, 2009



### More About This Article

Additional resources and features associated with this article are available within the HTML version:

- Supporting Information
- Links to the 6 articles that cite this article, as of the time of this article download
- Access to high resolution figures
- Links to articles and content related to this article
- Copyright permission to reproduce figures and/or text from this article

[View the Full Text HTML](#)

## Catalyzing the Translocation of Polypeptides through Attractive Interactions

Aaron J. Wolfe,<sup>†</sup> Mohammad M. Mohammad,<sup>†</sup> Stephen Cheley,<sup>‡</sup>  
Hagan Bayley,<sup>‡</sup> and Liviu Movileanu<sup>\*,†,§</sup>

Contribution from the Department of Physics, Syracuse University, 201 Physics Building, Syracuse, New York 13244-1130, Department of Chemistry, University of Oxford, Chemistry Research Laboratory, Mansfield Road, Oxford OX1 3TA, United Kingdom, and Structural Biology, Biochemistry, and Biophysics Program, Syracuse University, 111 College Place, Syracuse, New York 13244-4100

Received July 18, 2007; E-mail: lmovilea@physics.syr.edu

**Abstract:** Facilitated translocation of polypeptides through a protein pore is a ubiquitous and fundamental process in biology. Several translocation systems possess various well-defined binding sites within the pore lumen, but a clear mechanistic understanding of how the interaction of the polypeptides with the binding site alters the underlying kinetics is still missing. Here, we employed rational protein design and single-channel electrical recordings to obtain detailed kinetic signatures of polypeptide translocation through the *staphylococcal*  $\alpha$ -hemolysin ( $\alpha$ HL) transmembrane pore, a robust, tractable, and versatile  $\beta$ -barrel protein. Acidic binding sites composed of rings of negatively charged aspartic acid residues, engineered at strategic positions within the  $\beta$  barrel, produced dramatic changes in the functional properties of the  $\alpha$ HL protein, facilitating the transport of cationic polypeptides from one side of the membrane to the other. When two electrostatic binding sites were introduced, at the entry and exit of the  $\beta$  barrel, both the rate constants of association and dissociation increased substantially, diminishing the free energy barrier for translocation. By contrast, more hydrophobic polypeptides exhibited a considerable decrease in the rate constant of association to the pore lumen, having to overcome a greater energetic barrier because of the hydrophilic nature of the pore interior.

### Introduction

The significance of protein translocation through protein pores stems from the fact that approximately one-half of all proteins produced in a cell must, at some point, traverse a cellular membrane. Examples include not only several key processes involved in the cellular lifecycle,<sup>1–3</sup> but also the translocation of protein toxins through protein channels.<sup>4,5</sup> The present challenge rests on better defining the molecular mechanisms employed by protein translocase channels and establishing the broader biophysical rules that govern the transport of polypeptides. A transmembrane  $\beta$ -barrel is a common scaffold used by protein-conducting channels. The translocation of protein precursors into mitochondria and chloroplasts occurs through transmembrane  $\beta$ -barrel pores located in the outer membrane.<sup>6,7</sup>

For example, electrophysiological and circular dichroism studies of protein translocases from mitochondria (TOM)<sup>8,9</sup> and chloroplasts (TOC)<sup>10</sup> have indicated that these transmembrane proteins are  $\beta$ -barrel pores. A  $\beta$ -barrel pore may also serve as a passageway for enzymes to enter the cytosol, such as the lethal factor (LF) and the edema factor (EF), which unfold at least partially and translocate through a 14-stranded  $\beta$ -barrel formed by protective antigen channel (PA<sub>63</sub>) of anthrax toxin.<sup>4,5,11</sup>

Numerous fundamental questions surround the molecular mechanisms of the  $\beta$ -barrel translocases. What drives polypeptide transport? How do various traps or binding sites within the pore lumen catalyze the net flow of polypeptides? Can one control or anticipate the underlying translocation kinetics by rational design of either the  $\beta$ -barrel pore or the translocating polypeptide? All these specific questions generate a broader question regarding protein translocation: how do mitochondrial protein precursors move a significant distance into the organelle, traversing the translocase of the outer membrane (TOM) in the

<sup>†</sup> Department of Physics, Syracuse University.

<sup>‡</sup> University of Oxford.

<sup>§</sup> Structural Biology, Biochemistry, and Biophysics Program, Syracuse University.

- (1) Simon, S. M.; Peskin, C. S.; Oster, G. F. *Proc. Natl. Acad. Sci. U.S.A.* **1992**, *89*, 3770–3774.
- (2) Hessa, T.; Kim, H.; Bihlmaier, K.; Lundin, C.; Boekel, J.; Andersson, H.; Nilsson, I.; White, S. H.; von Heijne, G. *Nature* **2005**, *433*, 377–381.
- (3) Wickner, W.; Schekman, R. *Science* **2005**, *310*, 1452–1456.
- (4) Krantz, B. A.; Melnyk, R. A.; Zhang, S.; Juris, S. J.; Lacy, D. B.; Wu, Z.; Finkelstein, A.; Collier, R. J. *Science* **2005**, *309*, 777–781.
- (5) Krantz, B. A.; Finkelstein, A.; Collier, R. J. *J. Mol. Biol.* **2006**, *355*, 968–979.
- (6) Gabriel, K.; Buchanan, S. K.; Lithgow, T. *Trends Biochem. Sci.* **2001**, *26*, 36–40.

- (7) Matsuschek, A.; Glick, B. S. *Nat. Struct. Biol.* **2001**, *8*, 284–286.
- (8) Hill, K.; Model, K.; Ryan, M. T.; Dietmeier, K.; Martin, F.; Wagner, R.; Pfanner, N. *Nature* **1998**, *395*, 516–521.
- (9) Becker, L.; Bannwarth, M.; Meisinger, C.; Hill, K.; Model, K.; Krimmer, T.; Casadio, R.; Truscott, K. N.; Schulz, G. E.; Pfanner, N.; Wagner, R. *J. Mol. Biol.* **2005**, *353*, 1011–1020.
- (10) Hinnah, S. C.; Wagner, R.; Sveshnikova, N.; Harrer, R.; Soll, J. *Biophys. J.* **2002**, *83*, 899–911.
- (11) Karginov, V. A.; Nestorovich, E. M.; Moayeri, M.; Leppla, S. H.; Bezrukov, S. M. *Proc. Natl. Acad. Sci. U.S.A.* **2005**, *102*, 15075–15080.

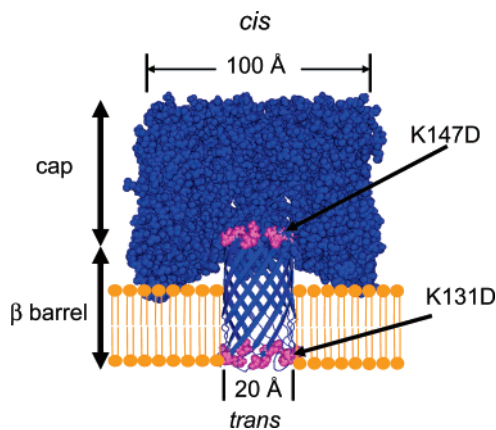


**Figure 1.** Molecular model of the  $\alpha$ HL protein pore highlighting the engineered acidic binding sites (in magenta) made of rings of aspartic acid (K131D<sub>7</sub> and K147D<sub>7</sub>). The model was built using PyMole<sup>25</sup> with the coordinates of 7ahl.pdb (Protein Data Bank).<sup>12</sup> K147 is located on the cis end of the  $\beta$  barrel, near the constriction region with a diameter of  $\sim 15$  Å. K131 is located on the trans side of the  $\beta$ -barrel, in a region of the lumen with a diameter of  $\sim 20$  Å, and is exposed to the aqueous phase.

absence of any energy-driven machinery? Previous studies using reconstituted lipid membranes have not clarified these long-standing questions owing to technical challenges, including the considerable complexity of the translocation machinery as well as a general lack of sufficient structural information.<sup>3</sup>

To overcome these difficulties, we adopted a strategy for implementing functionality into a  $\beta$ -barrel pore to facilitate polypeptide translocation. The obvious advantage of this methodology is not only to systematically test an array of hypotheses generated by the outstanding questions regarding protein translocation, but also to obtain the basic rules that govern this molecular process. *Staphylococcus aureus*  $\alpha$ -hemolysin ( $\alpha$ HL)<sup>12</sup> is a  $\beta$ -barrel pore that is similar in structure and size to many polypeptide-conducting  $\beta$ -barrel pores<sup>13</sup> and is also a versatile protein with an extraordinary stability under remodeling (Figure 1).<sup>14–17</sup> Additional advantages of this transmembrane protein pore are the availability of its high-resolution crystal structure,<sup>12</sup> its stability over long periods and under extreme environmental conditions,<sup>17,18</sup> and its large single-channel conductance,<sup>19</sup> facilitating high-resolution electrical recordings. Therefore, the  $\alpha$ HL protein was viewed to be an ideal candidate for the use as a model system to study the interactions between a translocating cationic polypeptide and a  $\beta$ -barrel protein pore via single-channel electrical recordings.

## Experimental Methods

**Construction of pT7- $\alpha$ HL-RL3.** pT7- $\alpha$ HL-RL3 encodes the WT- $\alpha$ HL polypeptide, but contains six silent restriction sites that encompass DNA encoding the transmembrane  $\beta$ -barrel. These sites are 5' to 3':

- (12) Song, L. Z.; Hobaugh, M. R.; Shustak, C.; Cheley, S.; Bayley, H.; Gouaux, J. E. *Science* **1996**, *274*, 1859–1866.
- (13) Schwartz, M. P.; Matouschek, A. *Proc. Natl. Acad. Sci. U.S.A.* **1999**, *96*, 13086–13090.
- (14) Howorka, S.; Movileanu, L.; Lu, X. F.; Magnon, M.; Cheley, S.; Braha, O.; Bayley, H. *J. Am. Chem. Soc.* **2000**, *122*, 2411–2416.
- (15) Movileanu, L.; Howorka, S.; Braha, O.; Bayley, H. *Nat. Biotechnol.* **2000**, *18*, 1091–1095.
- (16) Bayley, H.; Braha, O.; Cheley, S.; Gu, L. Q. Engineered nanopores. In *NanoBiotechnology*; Niemeyer, C. M. a. M. C. A., Ed.; Weinheim, Germany, 2004; pp 93–112.
- (17) Jung, Y.; Bayley, H.; Movileanu, L. *J. Am. Chem. Soc.* **2006**, *128*, 15332–15340.
- (18) Movileanu, L.; Cheley, S.; Bayley, H. *Biophys. J.* **2003**, *85*, 897–910.
- (19) Movileanu, L.; Schmittschmitt, J. P.; Scholtz, J. M.; Bayley, H. *Biophys. J.* **2005**, *89*, 1030–1045.

*SacII*, *HpaI*, *BsiWI*, *StuI*, *AflIII*, and *XhoI*. pT7- $\alpha$ HL-RL3 was derived from pT7- $\alpha$ HL-RL2<sup>20,21</sup> in two separate ligation steps. For the first step, pT7- $\alpha$ HL-RL2 was digested with *BsiWI* and *AflIII* and the purified vector was then ligated with two double-stranded oligonucleotide cassettes. The first cassette was formed from SC197, 5'GTACGGAT-TCAATGGTAATGTTACTGGTGATGATACAGGAAAA, and phosphorylated SC198, 5'AATTTTCTGTATCATCACCAGTAACAT-TACCATTGAATCC, while the second cassette was formed from phosphorylated SC199, 5'ATTGGAGGCCTTATTGGTGCAAAT-GTTTCGATTTCGTCATACAC, and SC200, 5'TTAAGTGTATGAC-GAATCGAAACATTTGCACCAATAAGGCCTCC. The resulting three-way ligation yielded pT7- $\alpha$ HL-RL3-K8A. In the second ligation step, the engineered Ala codon present in the  $\alpha$ HL-RL2 gene at position 8 was replaced with the wild-type Lys codon. To restore the wild-type residue, pT7- $\alpha$ HL-RL3-K8A was digested with *AgeI* and *MfeI*, and the resulting fragment was ligated with the wild-type gene in the T7 vector (pT7- $\alpha$ HL-WT) that had been cut with the same enzymes to yield pT7- $\alpha$ HL-RL3. All genes were verified by DNA sequencing.

**Construction of  $\beta$ -Barrel Mutants.  $\alpha$ HL-K131D<sub>7</sub>,  $\alpha$ HL-K147D<sub>7</sub>, and  $\alpha$ HL-K131D<sub>7</sub>/K147D<sub>7</sub>.** Mutant genes,  $\alpha$ HL-K131D<sub>7</sub> and  $\alpha$ HL-K147D<sub>7</sub>, were constructed by PCR-based recombination as previously described.<sup>22</sup> To construct  $\alpha$ HL-K131D<sub>7</sub>, pT7- $\alpha$ HL-RL3 (see above) was used as the template for PCR with mutagenic primers: SC807, 5'GGTGATGATACAGGAgacATTGGAGGCCTTATTGG (forward), and 5'SC808, 5'CCAATAAGGCCTCCAATgtcTCCTGTATCATCACC (reverse). The mutant codon and anticodon are in small type. For  $\alpha$ HL-K147D<sub>7</sub>, the mutagenic primers were SC809, 5'GGTCATACACTTgac-TATGTTCAACCTG (forward), and SC810, 5'CAGGTTGAACAT-AgtcAAGTGTATGACC (reverse). The non-mutagenic primers SC46, 5'ATAAAGTTGCAGGACCCTTCTG (forward), and SC47, 5'CA-GAAGTGGTCCTGCAACTTTAT (reverse), were used for both sets of PCR reactions. To construct the double aspartate mutant,  $\alpha$ HL-K131D<sub>7</sub>/K147D<sub>7</sub>, pT7- $\alpha$ HL-K147D<sub>7</sub> was digested with *StuI* and *HindIII*, and the resulting small fragment was ligated to the large fragment purified from pT7- $\alpha$ HL-K131D<sub>7</sub> after digestion with the same enzymes. Successful replacement was screened by cutting plasmid isolates with *AflIII*, since this site is removed by the K147D<sub>7</sub> mutation. All mutant genes were verified by DNA sequencing.

**Polypeptide Synthesis and Purification.** The polypeptides used in this work were Syn B2 = MLSRQQSQRQSRQSRQSRQSRYL (HPLC purity was 95.0%,  $M_w$  = 2893.3 Da), Cox IV = MLSLRQSIRFFK-PATRLTLCSSRY (90.1%, 2762.3Da) and AK = (AAKAA)<sub>5</sub>Y-NH<sub>2</sub> (96.4%, 2243.7 Da). The polypeptides were synthesized by an automatic solid-phase method using an active ester coupling procedure with Fmoc-amino acids, purified by reversed-phase HPLC, and confirmed by MALDI-TOF mass spectrometry and analytical HPLC (GenScript corporation, Scotch Plains, NJ).

**Mutant  $\alpha$ HL Pores.** [<sup>35</sup>S]methionine-labeled, mutant  $\alpha$ HL polypeptides were synthesized and assembled in vitro by coupled transcription and translation (IVTT) in the presence of rabbit erythrocyte membranes as previously described.<sup>23</sup> The labeled, membrane-bound homoheptamers were washed in MBSA buffer (10 mM MOPS; titrated with NaOH, 150 mM NaCl, containing 0.1% (wt/v) BSA, pH 6.8), solubilized in sample buffer,<sup>24</sup> and then purified on an 8% SDS-polyacrylamide gel. The gel was then dried between two sheets of plastic film (catalog no. V713B; Promega Corporation) at 50 °C for 2 h using a Bio-Rad drying system ("GelAir" catalog no. 165–1771, Bio-Rad Laboratories). After autoradiography of the dried gel, bands corresponding to each mutant oligomer were excised with scissors and

- (20) Cheley, S.; Braha, G.; Lu, X. F.; Conlan, S.; Bayley, H. *Protein Sci.* **1999**, *8*, 1257–1267.
- (21) Movileanu, L.; Bayley, H. *Proc. Natl. Acad. Sci. U.S.A.* **2001**, *98*, 10137–10141.
- (22) Howorka, S.; Bayley, H. *Biotechniques* **1998**, *25*, 764.
- (23) Movileanu, L.; Cheley, S.; Howorka, S.; Braha, O.; Bayley, H. *J. Gen. Physiol.* **2001**, *117*, 239–251.
- (24) Laemmli, U. K. *Nature* **1970**, *227*, 680–685.

rehydrated in 0.5 mL of ultrapure, distilled, and deionized water. The adherent, plastic gel-backings were released from the slices after rehydration and removed with flamed-metal forceps prior to maceration with a disposable plastic pestle (catalog no. 749521-1590; Nalge Nunc International). Gel fragments were removed with a spin filter ("QIASHredder", catalog no. 79654; Qiagen), and the resulting filtrate was stored frozen in 50  $\mu$ L aliquots at  $-80^{\circ}\text{C}$ .

**Molecular Graphics.** The  $\alpha$ HL model (7ahl.pdb) was generated with the PyMol software package.<sup>25</sup>

**Electrical Recordings in Planar Bilayers.** Electrical recordings were carried out with planar bilayer lipid membranes.<sup>21,26</sup> The *cis* and *trans* chambers of the apparatus were separated by a 25  $\mu\text{m}$ -thick Teflon septum (Goodfellow Corporation, Malvern, PA). A 1,2 diphytanoyl-*sn*-glycerophosphatidylcholine (Avanti Polar Lipids, Alabaster, AL) bilayer was formed across a 60  $\mu\text{m}$ -wide aperture in the septum. The electrolyte in both chambers was 1 M KCl, 10 mM potassium phosphate, pH 7.4. The  $\alpha$ HL pores were introduced by adding gel-purified homoheptamers (0.5–2.0  $\mu\text{L}$ ) to the *cis* chamber, to give a final protein concentration of 0.05–0.2 ng/mL. Single-channel currents were recorded by using a patch clamp amplifier (Axopatch 200B, Axon Instruments, Foster City, CA) connected to Ag/AgCl electrodes through agar bridges. The *cis* chamber was grounded and a positive current (upward deflection) represents positive charge moving from the *trans* to *cis* side. A Pentium PC was equipped with a DigiData 1322A A/D converter (Axon) for data acquisition. The signal was low-pass filtered with an 8-pole Bessel filter at a frequency of 10 kHz and sampled at 50 kHz, unless otherwise stated. For data acquisition and analysis, we used the pClamp9.2 software package (Axon).

## Results

**Design of the Binding Sites.** Our major hypothesis was that acidic binding sites engineered within the pore lumen would produce a major alteration in the polypeptide permeability of the  $\alpha$ HL protein pore. We designed two mutants containing a binding site located either at the *trans* entrance of the pore lumen, at position 131, or near the constriction region of the  $\beta$  barrel, at position 147 (Figure 1). In both mutants, a lysine was replaced by an aspartic acid. Because of the stoichiometry of the  $\alpha$ HL protein pore, each single-site mutation in the monomer resulted in seven-residue replacements in the heptameric pore, creating an acidic iris composed of aspartic acid side chains. In this way, a single-site mutation introduced a  $-14$  net charge in the fully assembled pore (K131D<sub>7</sub> or K147D<sub>7</sub>, Figure 1). To reveal the cumulative effect of both acidic binding sites, we further designed a double-site mutant, K131D<sub>7</sub>/K147D<sub>7</sub>, which introduced a  $-28$  net charge alteration in the lumen of the  $\alpha$ HL pore. Replacement of Lys with Asp near the constriction region of the pore lumen modified the permeability properties of the  $\alpha$ HL pore from a slightly anion-selective to a cation-selective channel. For example, the permeability ratio  $P_{\text{K}}/P_{\text{Cl}}$  was  $0.71 \pm 0.05$  ( $n = 3$ ) for the wild-type  $\alpha$ HL (WT- $\alpha$ HL) pore, in accord with previous studies.<sup>27</sup> The K131D<sub>7</sub>, K147D<sub>7</sub>, and K131D<sub>7</sub>/K147D<sub>7</sub> pores exhibited a permeability ratio  $P_{\text{K}}/P_{\text{Cl}}$  of  $0.71 \pm 0.12$  ( $n = 3$ ),  $1.43 \pm 0.13$  ( $n = 3$ ), and  $4.50 \pm 0.97$  ( $n = 3$ ), respectively (Supporting Information, Figure S1, Table S1).

**Single-Channel Electrical Recordings of the Wild-Type and Engineered  $\alpha$ HL Pores in the Presence of Cationic Polypeptides.** Single-channel electrical recordings<sup>28,29</sup> were

(25) Delano, W. L. *DeLano Scientific*; DeLano Scientific: San Carlos, CA, 2007.  
 (26) Miles, G.; Movileanu, L.; Bayley, H. *Protein Sci.* **2002**, *11*, 894–902.  
 (27) Gu, L. Q.; Dalla Serra, M.; Vincent, J. B.; Vigh, G.; Cheley, S.; Braha, O.; Bayley, H. *Proc. Natl. Acad. Sci. U.S.A.* **2000**, *97*, 3959–3964.

**Table 1.** Biophysical Properties of the Cationic Polypeptides

polypeptide <sup>a</sup>	length (residues)	charge <sup>b</sup>	fractional helicity <sup>c</sup> (%)	Kyte–Doolittle hydrophathy index <sup>d</sup>
AK	26	+5	17.4	15.2
Cox IV	23	+5	5	−5.2
Syn B2	23	+5	12	−44.4

<sup>a</sup> The sequences of the polypeptides are presented in the section Materials and Methods. <sup>b</sup> The charge is estimated at pH 7.4. <sup>c</sup> Fractional helicity is calculated as previously described.<sup>19</sup> <sup>d</sup> The positive numbers indicate the hydrophobic feature of the polypeptide, whereas the negative numbers indicate their hydrophilic nature. These values represent the sums of the Kyte–Doolittle hydrophathy indexes for the individual amino acids in the polypeptide.<sup>31</sup>

carried out to examine the interaction of various cationic polypeptides with the WT- $\alpha$ HL and engineered  $\alpha$ HL pores. Three selected polypeptides were explored: an alanine-based polypeptide AK with the repeat unit AAKAA, a mitochondrial presequence Cox IV, and a synthetic hydrophilic presequence Syn B2.<sup>10,30</sup> These polypeptides were closely similar in length ( $\sim 25$  residues) and charge (ca. +5) at pH 7.4, but they differed greatly in their hydrophathy index: 15.2,  $-5.2$ , and  $-44.4$ , respectively (Table 1).<sup>31</sup> When inserted into a planar lipid bilayer, all four channels investigated here remained open for long periods (Supporting Information, Figure S2). By contrast, when the cationic polypeptides were added to the *trans* side, at low micromolar concentrations, transient current blockades were observed, the nature of which was dependent on both the features of the engineered  $\alpha$ HL pore as well as the translocating polypeptides (Figure 2, Supporting Information, Tables S2–S4). For the simplicity of further data interpretations, our single-channel experiments were performed with the polypeptide analyte added only to the *trans* side. This is motivated by the fact that a significant part of the  $\alpha$ HL protein ( $\sim 50$  Å) protrudes within the *cis* aqueous phase (Figure 1).<sup>12</sup> In other words, the polypeptide analyte added to the *cis* chamber would undergo a significant entropic penalty within the voltage-independent part of the pore lumen<sup>32,33</sup> before its partitioning into the voltage-dependent transmembrane  $\beta$ -barrel part.

Figure 2 illustrates the effect of the Syn B2 polypeptide on the single-channel electrical signature of the WT- $\alpha$ HL and engineered  $\alpha$ HL protein pores. A log likelihood ratio (LLR) test<sup>18,19</sup> of dwell-time histograms showed a two-exponential distribution of the transient current blockades produced by the cationic polypeptides in single-channel recordings with the WT- $\alpha$ HL pore. At a transmembrane potential of +80 mV, we observed transient current blockades with two durations:  $\tau_{\text{off-1}} = 0.9 \pm 0.4$  ms, with a frequency  $f_1 = 11 \pm 4$  s<sup>-1</sup> (the short-lived events), and  $\tau_{\text{off-2}} = 2.7 \pm 0.1$  ms, with  $f_2 = 15 \pm 5$  s<sup>-1</sup> (the long-lived events,  $n = 3$ ) (Figure 2A). The short-lived current blockades (denoted by the subscript "1") were not voltage dependent, and we interpreted them as transient collisions of the cationic polypeptides with the *trans* opening of the  $\alpha$ HL pores (data not shown). Therefore, they were neglected in the further determination of the kinetic constants. The long-

(28) Sackmann, B.; Neher, E. *Single-Channel Recording*; Kluwer Academic/Plenum Publishers: New York, 1995.

(29) Hille, B. *Ion Channels of Excitable Membranes*; Sinauer Associates, Inc.: Sunderland, MA, 2001.

(30) Muro, C.; Grigoriev, S. M.; Pietkiewicz, D.; Kinnally, K. W.; Campo, M. L. *Biophys. J.* **2003**, *84*, 2981–2989.

(31) Kyte, J.; Doolittle, R. F. *J. Mol. Biol.* **1982**, *157*, 105–132.

(32) Howorka, S.; Movileanu, L.; Braha, O.; Bayley, H. *Proc. Natl. Acad. Sci. U.S.A.* **2001**, *98*, 12996–13001.

(33) Howorka, S.; Bayley, H. *Biophys. J.* **2002**, *83*, 3202–3210.

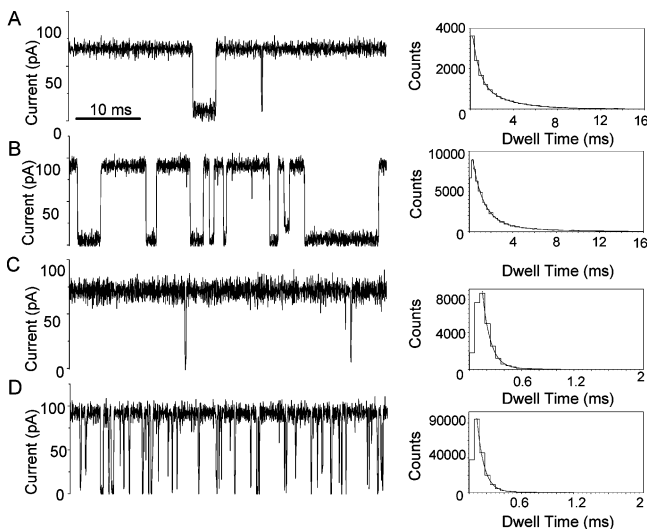


**Figure 2.** Representative single-channel electrical recordings with the wild-type and engineered  $\alpha$ HL protein pores in the presence of 34  $\mu$ M of the Syn B2 polypeptide added to the *trans* side: (A) WT- $\alpha$ HL, (B) K131D<sub>7</sub>, (C) K147D<sub>7</sub>, (D) K131D<sub>7</sub>/K147D<sub>7</sub>. The frequency and duration of the polypeptide-induced current blockades were dependent on the position of the engineered binding site. All traces were recorded in symmetrical buffer conditions (1 M KCl and 10 mM potassium phosphate, pH 7.4) at +80 mV. The smooth curves from the right-handed histograms were either double-exponential (for A and B) or single-exponential (for C and D) fits (details are provided in the main text and Supporting Information, Table S2). The single-channel electrical traces were low-pass Bessel filtered at 2 kHz.

lived events (denoted by the subscript “2”) were voltage dependent and were attributed to major partitioning of the polypeptides into the pore lumen.<sup>19</sup> Highly frequent current blockades were observed with the K131D<sub>7</sub> pore ( $\tau_{\text{off-1}} = 0.31 \pm 0.06$  ms,  $f_1 = 100 \pm 20$  s<sup>-1</sup>; and  $\tau_{\text{off-2}} = 3.0 \pm 0.04$  ms,  $f_2 = 29 \pm 11$  s<sup>-1</sup>,  $n = 3$ ) (Figure 2B). Furthermore, in contrast to WT- $\alpha$ HL and K131D<sub>7</sub>, the short-lived events were not observed with K147D<sub>7</sub> ( $\tau_{\text{off-2}} = 0.14 \pm 0.02$  ms,  $f_2 = 47 \pm 1$  s<sup>-1</sup>,  $n = 3$ ) and K131D<sub>7</sub>/K147D<sub>7</sub> ( $\tau_{\text{off-2}} = 0.091 \pm 0.005$  ms,  $f_2 = 400 \pm 17$  s<sup>-1</sup>,  $n = 3$ , Figure 2C,D), as judged by a log likelihood ratio test. One simple interpretation for the assignment of the short-lived events “1” is that the interaction of the polypeptide with the *trans* opening of the pore is more than a simple collision, but rather is likely accompanied by other complex electrostatic interactions. As the *trans* opening is the same for all  $\alpha$ HL pores examined in this work, transient short-lived conformational fluctuations of the positively charged polypeptide within the pore lumen would allow its trapping by the negatively charged binding site located at position 147.

**Determination of the Kinetic Constants.** We found that the reciprocal of  $\tau_{\text{on}}$  (the mean inter-event interval) is linearly dependent on the polypeptide concentration, whereas  $\tau_{\text{off}}$  (the mean dwell time from the histogram of the occupied states) is independent of the polypeptide concentration (data not shown). Thus, a simple bimolecular interaction between the polypeptide and the pore can be assumed. The rate constants of association  $k_{\text{on}}$  were derived from the slopes of plots of  $1/\tau_{\text{on}}$  versus [polypeptide], where [polypeptide] is the polypeptide concentration in the aqueous phase. The rate constants of dissociation ( $k_{\text{off}}$ ) were determined by averaging the  $1/\tau_{\text{off}}$ .

The cationic polypeptide exits the  $\alpha$ HL pore through either the *trans* or *cis* opening, so that the total rate constant of dissociation was defined as  $k_{\text{off-2}} = k_{\text{off-2}}^{\text{cis}} + k_{\text{off-2}}^{\text{trans}}$ , where

$k_{\text{off-2}} = 1/\tau_{\text{off-2}}$ , and  $\tau_{\text{off-2}}$  is the mean dwell time of the long-lived events.<sup>19</sup> The voltage dependence of the rate constant of dissociation  $k_{\text{off-2}}$  underwent a crossover behavior, indicating the transition from the *trans*- to *cis*-mediated dissociation. Accordingly,  $k_{\text{off-2}}$  was fitted by a sum of two exponentials that resulted from the combination of  $k_{\text{off-2}}^{\text{cis}}$  and  $k_{\text{off-2}}^{\text{trans}}$ .<sup>19</sup> This analysis provides various fundamental parameters that describe the translocation mechanism, including the *cis* ( $k_{\text{off-2}}^{\text{cis}}$ ) and *trans* ( $k_{\text{off-2}}^{\text{trans}}$ ) rate constants of dissociation at a certain transmembrane potential and their corresponding fractional rate constants of association  $k_{\text{on-2}}^{\text{trans}}$  and  $k_{\text{on-2}}^{\text{cis}}$ . These rate constants were calculated as  $P_{\text{on-2}}^{\text{trans}} \times k_{\text{on-2}}$  and  $P_{\text{on-2}}^{\text{cis}} \times k_{\text{on-2}}$ , respectively.<sup>19</sup> The probability of the polypeptide to exit the pore through the *trans* and *cis* opening was calculated as  $P_{\text{on-2}}^{\text{trans}} = k_{\text{off-2}}^{\text{trans}}/k_{\text{off-2}}$  and  $P_{\text{on-2}}^{\text{cis}} = k_{\text{off-2}}^{\text{cis}}/k_{\text{off-2}}$ , respectively. Also  $k_{\text{on-2}} = k_{\text{on-2}}^{\text{trans}} + k_{\text{on-2}}^{\text{cis}}$ , where  $k_{\text{on-2}} = 1/([\text{polypeptide}]\tau_{\text{on-2}})$ .

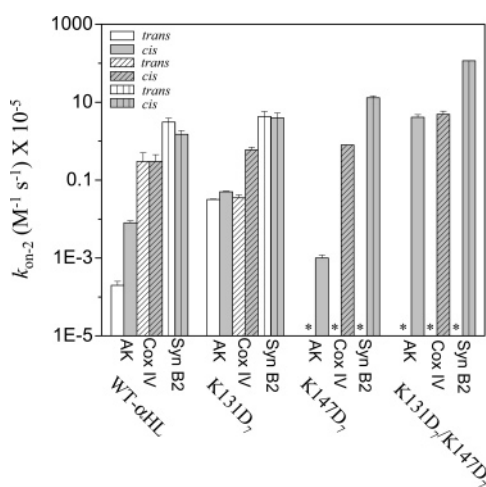
**The Rate Constants of Association ( $k_{\text{on-2}}$ ).** Remarkably, the rate constants of association ( $k_{\text{on-2}}$ ) spanned at least 5 orders of magnitude and exhibited a well-defined pattern with the nature of the pore and the cationic polypeptide (Table 2).  $k_{\text{on-2}}$  exponentially decreased with the transmembrane potential, suggesting a voltage-dependent single-barrier profile for the rate constant of association. Interestingly,  $k_{\text{on-2}}$  increased with the hydrophilic feature of the polypeptides in the following sequence: AK < Cox IV < Syn B2, and for all pores (Table 2). In Figure 3, we show both fractional rates of association,  $k_{\text{on-2}}^{\text{cis}}$  and  $k_{\text{on-2}}^{\text{trans}}$ , that correspond to the exit of the polypeptides across the *cis* and *trans* opening of the  $\alpha$ HL pore, respectively. At a transmembrane potential of +80 mV,  $k_{\text{on-2}}^{\text{cis}}$  was dominant for the K147D<sub>7</sub> and K131D<sub>7</sub>/K147D<sub>7</sub> pores (Figure 3). This finding indicates that the exit of the polypeptides primarily occurred across the *cis* opening of the pore when the binding site K147D was present. Therefore, the position of the binding site qualitatively altered the net flux of cationic polypeptides through the  $\alpha$ HL pore. For Syn B2 and Cox IV, the values of  $k_{\text{on-2}}^{\text{cis}}$  calculated for the K147D<sub>7</sub> pore moderately increased compared to those values corresponding to the WT- $\alpha$ HL pore. In contrast,  $k_{\text{on-2}}^{\text{cis}}$  for the K131D<sub>7</sub>/K147D<sub>7</sub> pore values were substantially greater than the values obtained with the WT- $\alpha$ HL pore (Table 2, Figure 3), suggesting that two binding sites, at the entry and exit of the pore, synergistically enhance the net flux of cationic polypeptides through the  $\alpha$ HL pore from the *trans* to *cis* side.

**The Rate Constants of Dissociation ( $k_{\text{off-2}}$ ).** Similar with the previous study employing alanine-based polypeptides,<sup>19</sup> we fitted the  $k_{\text{off-2}}(V)$ , where  $V$  is the transmembrane potential, with a two-exponential function that can be attributed to a two-barrier-free energy landscape; the first barrier corresponds to the activation-free energy of the polypeptide to exit the pore through the *trans* side ( $k_{\text{off-2}}^{\text{trans}}$ ), whereas the second barrier corresponds to the activation-free energy of the polypeptide to exit the pore through the *cis* side ( $k_{\text{off-2}}^{\text{cis}}$ ). Therefore, in a linear plot, the  $k_{\text{off-2}}(V)$  showed a biphasic profile with a minimum that corresponded to a critical value of the transmembrane potential ( $V_c$ ). For  $V > V_c$ , polypeptide exit through the *cis* side is energetically favorable ( $k_{\text{off-2}}^{\text{cis}} > k_{\text{off-2}}^{\text{trans}}$ ), and vice-versa for  $V < V_c$ . In Figure 4, we show the rate constants of dissociation ( $k_{\text{off-2}}$ ), normalized to the value that corresponds to +20 mV, in a semilogarithmic plot versus the transmembrane

**Table 2.** The Rate Constants of Association  $k_{\text{on}-1}$ ,  $k_{\text{on}-2}$ ,  $k_{\text{on}-2}^{\text{trans}}$ , and  $k_{\text{on}-2}^{\text{cis}}$  of the Interaction between Cationic Polypeptides and  $\alpha$ HL Pores at a Transmembrane Potential of +80 mV<sup>a</sup>

peptide	pore	$k_{\text{on}-1}$ ( $\text{M}^{-1}\text{s}^{-1}$ ) $\times 10^{-5}$	$k_{\text{on}-2}$ ( $\text{M}^{-1}\text{s}^{-1}$ ) $\times 10^{-5}$	$k_{\text{on}-2}^{\text{trans}}$ ( $\text{M}^{-1}\text{s}^{-1}$ ) $\times 10^{-5}$	$k_{\text{on}-2}^{\text{cis}}$ ( $\text{M}^{-1}\text{s}^{-1}$ ) $\times 10^{-5}$
Syn B2	WT- $\alpha$ HL	3.2 $\pm$ 1.3	4.4 $\pm$ 1.3	3.1 $\pm$ 0.8	1.5 $\pm$ 0.4
	K131D <sub>7</sub>	29 $\pm$ 6	8.5 $\pm$ 2.6	4.3 $\pm$ 1.5	4.0 $\pm$ 1.3
	K147D <sub>7</sub>	N/A <sup>b</sup>	13.8 $\pm$ 6.8	<0.014 <sup>c</sup>	13.0 $\pm$ 1.6
	K131D <sub>7</sub> /K147D <sub>7</sub>	N/A <sup>b</sup>	117 $\pm$ 1	< 0.12 <sup>c</sup>	116 $\pm$ 1
Cox IV	WT- $\alpha$ HL	0.20 $\pm$ 0.02	0.60 $\pm$ 0.03	0.3 $\pm$ 0.2	0.30 $\pm$ 0.15
	K131D <sub>7</sub>	0.3 $\pm$ 0.1	0.90 $\pm$ 0.15	0.035 $\pm$ 0.007	0.6 $\pm$ 0.1
	K147D <sub>7</sub>	N/A <sup>b</sup>	0.80 $\pm$ 0.03	< 0.0008 <sup>c</sup>	0.8 $\pm$ 0.2
	K131D <sub>7</sub> /K147D <sub>7</sub>	N/A <sup>b</sup>	5.0 $\pm$ 0.1	< 0.0045 <sup>c</sup>	4.9 $\pm$ 0.1
AK	WT- $\alpha$ HL	0.04 $\pm$ 0.01	0.008 $\pm$ 0.002	0.00020 $\pm$ 0.00005	0.008 $\pm$ 0.001
	K131D <sub>7</sub>	0.20 $\pm$ 0.07	0.08 $\pm$ 0.01	0.032 $\pm$ 0.001	0.050 $\pm$ 0.002
	K147D <sub>7</sub>	0.17 $\pm$ 0.01	0.001 $\pm$ 0.0002	<0.0000008 <sup>c</sup>	0.0010 $\pm$ 0.0002
	K131D <sub>7</sub> /K147D <sub>7</sub>	N/A <sup>b</sup>	4.1 $\pm$ 0.73	<0.004 <sup>c</sup>	4.1 $\pm$ 0.7

<sup>a</sup> All experiments were carried out in symmetrical conditions of 1 M KCl, 10 mM potassium phosphate, pH 7.4. A 34  $\mu\text{M}$  portion of polypeptide was added to the *trans* chamber. The values represent means  $\pm$  SDs calculated from three separate single-channel experiments. <sup>b</sup> The short-lived voltage-independent events “1” were undetectable. <sup>c</sup> The numbers represent the upper limit of the rate constant of association based upon a probability lower than 0.1%.

**Figure 3.** The rate constants of association  $k_{\text{on}-2}^{\text{trans}}$  and  $k_{\text{on}-2}^{\text{cis}}$  calculated for a transmembrane potential of +80 mV. The other conditions are the same as those mentioned in Figure 2. The missing bars indicated by “\*” have a value less than 0.1%  $k_{\text{on}-2}$  (Table 2). The values represent means  $\pm$  SDs calculated from three separate single-channel experiments.

potential (V). In the range of the transmembrane potential of 20–100 mV,  $k_{\text{off}-2}$  decreased with an increase in V for the WT- $\alpha$ HL pore regardless of the polypeptide, suggesting that the pore lacking the binding site(s) is poorly permeable for cationic polypeptides. In contrast,  $k_{\text{off}-2}$  increased with an increase in V for the K131D<sub>7</sub>/K147D<sub>7</sub> pore (Figure 4), indicating an enhanced permeability for cationic polypeptides, which is in accord with the absence of the short-lived events “1” noticed with all polypeptides examined in this work. Table 3 illustrates the values of the rate constants of dissociation  $k_{\text{off}-1}$ ,  $k_{\text{off}-2}$ ,  $k_{\text{off}-2}^{\text{trans}}$  and  $k_{\text{off}-2}^{\text{cis}}$  for all cases examined here. The rate constants of dissociation ( $k_{\text{off}-2}$ ) determined for the K147D<sub>7</sub> and K131D<sub>7</sub>/K147D<sub>7</sub> pores were generally greater than those values corresponding to the WT- $\alpha$ HL and K131D<sub>7</sub> pores, primarily because of a substantial increase in the rate constant of dissociation through the *cis* opening of the pore ( $k_{\text{off}-2}^{\text{cis}}$ , Table 3). For the K147D<sub>7</sub> and K131D<sub>7</sub>/K147D<sub>7</sub> pores, the values of  $k_{\text{off}-2}^{\text{trans}}$  were negligible, indicating a facilitated flow of cationic polypeptides from the *trans* to *cis* side of the membrane, which is in excellent agreement with our hypothesis.

## Discussion

**$\beta$ -Barrels with a Single Attractive Trap.** In this work, we obtained a highly detailed kinetic signature of the translocation of cationic polypeptides through a transmembrane  $\beta$ -barrel pore containing negatively charged binding sites engineered within the pore lumen. For a binding site located within the  $\beta$  barrel, we found that its position qualitatively alters the flow of polypeptides. This situation is similar to that of a selective ion channel containing a binding site for a particular type of small ions, such as sodium or potassium.<sup>34–36</sup> The polypeptide flux through a binding site-containing  $\alpha$ HL pore is greater than that through a wild-type  $\alpha$ HL pore (Table 2).

By comparison with WT- $\alpha$ HL, K131D<sub>7</sub> exhibited an increase of the rate constant of association ( $k_{\text{on}-2}$ ). The high rate constant of association is consistent with the location of the binding site near the side of greater polypeptide concentration (Figures 1, 3). Except for the hydrophobic polypeptide AK,  $k_{\text{on}-2}$  is higher with the K147D<sub>7</sub> and K131D<sub>7</sub>/K147D<sub>7</sub> pores than with the WT- $\alpha$ HL pore. The WT- $\alpha$ HL pore has a “steric” binding site for polypeptides, near the constriction region.<sup>19</sup> Previous work on the interactions between the cationic alanine-based polypeptides and the  $\alpha$ HL pore showed that the overall free energy landscape can be depicted by a two-barrier, single-well profile.<sup>19</sup>

We interpret these results in terms of the alteration of the free energy barrier for polypeptide translocation. The first barrier (“the entry barrier”) is determined by the energetic cost of the polypeptides for their partitioning from aqueous phase into the pore lumen. The second barrier (“the exit barrier”) is determined by the energetic cost of the polypeptides required to traverse the constriction of the  $\alpha$ HL pore near the *cis* end of the  $\beta$  barrel. The acidic binding sites, either at position 131 or 147, add an additional “attractive” binding site that alters either “the entry or exit barrier,” respectively. For example, the polypeptides translocate faster through the K147D<sub>7</sub> pore than through the WT- $\alpha$ HL pore ( $k_{\text{off}-2}^{\text{cis}}$ , Table 3, Figure 2), resulting in a significantly reduced “exit barrier” through the *cis* end of the  $\beta$  barrel. We propose that both negatively charged binding sites

- (34) Berezhkovskii, A. M.; Bezrukov, S. M. *Biophys. J.* **2005**, *88*, L17–L19.  
 (35) Bauer, W. R.; Nadler, W. J. *Chem. Phys.* **2005**, *122*.  
 (36) Bauer, W. R.; Nadler, W. *Proc. Natl. Acad. Sci. U.S.A.* **2006**, *103*, 11446–11451.

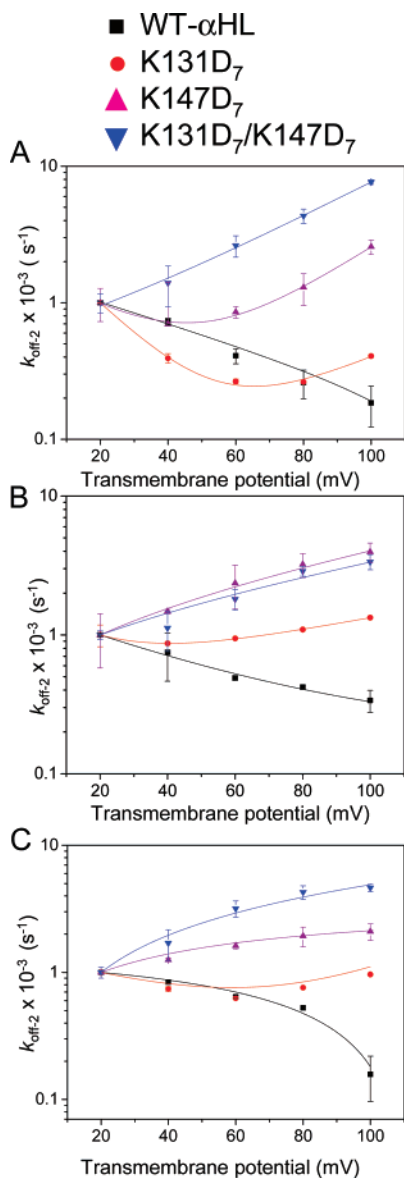


**Figure 4.** Voltage-dependence of the rate constants of dissociation ( $k_{\text{off}-2}$ ) normalized to that value corresponding to +20 mV and fitted with a two-exponential function:<sup>19</sup> (A) the Syn B2 polypeptide, (B) the Cox IV mitochondrial polypeptide in the presence of 100  $\mu\text{M}$  DTT, (C) the AK polypeptide. All experiments were carried out in symmetrical buffer conditions (1 M KCl, 10 mM potassium phosphate, pH 7.4). A 34  $\mu\text{M}$  portion of polypeptide was added to the *trans* side of the bilayer. The values represent means  $\pm$  SDs calculated from three separate single-channel experiments.

have a catalytic role in translocating the polypeptides from one side of the membrane to the other.

Alternatively, the kinetic data obtained from single-channel recordings can be interpreted in the light of the occupation probability  $n$  and the first passage time  $\tau_{\text{off}-2}$  to traverse the  $\alpha\text{HL}$  pore.<sup>35,36</sup> In this work, the experiments were performed at low micromolar concentration of cationic polypeptides. Under these conditions, the reciprocal of  $\tau_{\text{on}-2}$  is proportional to the concentration of polypeptide, indicating that complex interactions between polypeptides due to the polypeptide-induced current blockades are negligible. Therefore, the flow of polypeptides through the  $\alpha\text{HL}$  pore is  $J = n[\text{polypept}]/\tau_{\text{off}-2}$ .<sup>35,36</sup> The transmembrane potential implies the superposition of an attractive potential with the native interaction potential between the

polypeptide and the protein pore.<sup>19</sup> This superposition produces an increase in the occupation number  $n$ , which is in accord with our experimental findings, because the flow of polypeptides  $J$  increases with the occupation number. On the other hand, the engineered trap at position 147 dramatically reduces  $\tau_{\text{off}-2}$  (Figures 2-4), increasing the flow of the translocating polypeptides. Finally, the two engineered traps, at the entry (K131D) and the exit (K147D) of the  $\beta$  barrel, increase the occupation number  $n$  and decrease the first passage time  $\tau_{\text{off}-2}$ , respectively, substantially enhancing the flow of translocating polypeptides (Figures 2-4).

This work demonstrates that an electrostatic interaction between the translocating polypeptides and the pore lumen is a determining factor that facilitates their transport. Intuitively, a very strong interaction between the translocating polypeptide and the pore lumen is accompanied by a much longer residence time inside the pore, which will reduce the net flux of polypeptides. This could be reasoned by the facts that (i) polypeptides bound temporarily inside the pore might hamper the translocation of other polypeptides by blocking the channel and (ii) the interaction is so strong that the polypeptide exits the pore through the *trans* opening. In this paper, we did not examine the effect of the strength of the binding interaction on the transport of polypeptides, and this issue remains to be clarified in a future study.

**Why Two Traps Are Better Than One.** Compared with WT- $\alpha\text{HL}$ , the rate constants of association ( $k_{\text{on}-2}$ ) and dissociation ( $k_{\text{off}-2}$ ) increased for the double mutant (Tables 2-3). This situation is different from that observed with the K147D<sub>7</sub> pore in which only the  $k_{\text{off}-2}$  rate constant was increased or that observed with the K131D<sub>7</sub> pore in which only the  $k_{\text{on}-2}$  rate constant was increased (Tables 2-3). Together, the 131 and 147 binding sites have a synergistic effect by increasing both  $k_{\text{on}-2}$  and  $k_{\text{off}-2}$ . We propose that both binding sites act as a Brownian ratchet pulling successive fragments of the translocating polypeptide through attractive electrostatic forces. These results show that the kinetics of polypeptide translocation through an engineered  $\alpha\text{HL}$  pore is dramatically altered by comparison with the WT- $\alpha\text{HL}$  pore, and is dependent on the position of the binding site.

This data may offer an explanation why the TOM channel possesses two major acidic binding sites, one at the entry of the barrel, and one at its exit, protruding into the intermembrane surface.<sup>37</sup> The presequence-containing proteins traverse the TOM channels in the absence of any ATP or energy-driven cellular factor and with an enormous entropic cost.<sup>3</sup> Positively charged presequences interact with the negatively charged binding sites within the TOM channels, resulting in electrostatic forces required to guide the translocating proteins across the outer membrane of mitochondria. The binding sites at the entry and exit of the TOM channel reduce the activation free energy of the polypeptides to partition into the channel through the cytosolic opening and to escape the channel through the opposite opening, respectively. For example, removal of the acidic binding site at the intermembrane surface inhibited protein import 3 to 8-fold.<sup>38</sup> By analogy, the results obtained with the K131D<sub>7</sub>/K147D<sub>7</sub> pore provide strong evidence for a substantial

(37) Chacinska, A.; Pfanner, N.; Meisinger, C. *Trends Cell Biol.* **2002**, *12*, 299-303.

(38) Bolliger, L.; Junne, T.; Schatz, G.; Lithgow, T. *EMBO J.* **1995**, *14*, 6318-6326.

**Table 3.** The Rate Constants of Dissociation  $k_{\text{off}-1}$ ,  $k_{\text{off}-2}$ ,  $k_{\text{off}-2}^{\text{trans}}$ , and  $k_{\text{off}-2}^{\text{cis}}$  of the Interaction between Cationic Polypeptides and  $\alpha$ HL Pores at a Transmembrane Potential of +80 mV<sup>a</sup>

peptide	protein pore	$k_{\text{off}-1}$ ( $\text{s}^{-1}$ ) $\times 10^{-3}$	$k_{\text{off}-2}$ ( $\text{s}^{-1}$ ) $\times 10^{-3}$	$k_{\text{off}-2}^{\text{trans}}$ ( $\text{s}^{-1}$ ) $\times 10^{-3}$	$k_{\text{off}-2}^{\text{cis}}$ ( $\text{s}^{-1}$ ) $\times 10^{-3}$
Syn B2	WT- $\alpha$ HL	1.1 $\pm$ 0.4	0.37 $\pm$ 0.02	0.29 $\pm$ 0.01	0.14 $\pm$ 0.01
	K131D <sub>7</sub>	3.2 $\pm$ 2.0	0.33 $\pm$ 0.04	0.20 $\pm$ 0.03	0.12 $\pm$ 0.02
	K147D <sub>7</sub>	N/A <sup>b</sup>	7.2 $\pm$ 1.2	N/A <sup>c</sup>	7 $\pm$ 2
	K131D <sub>7</sub> /K147D <sub>7</sub>	N/A <sup>b</sup>	11 $\pm$ 1	N/A <sup>c</sup>	10 $\pm$ 1
Cox IV	WT- $\alpha$ HL	0.76 $\pm$ 0.01	0.11 $\pm$ 0.01	0.050 $\pm$ 0.002	0.052 $\pm$ 0.002
	K131D <sub>7</sub>	2.1 $\pm$ 1.3	0.16 $\pm$ 0.04	0.15 $\pm$ 0.04	0.009 $\pm$ 0.003
	K147D <sub>7</sub>	N/A <sup>b</sup>	4.8 $\pm$ 0.6	N/A <sup>c</sup>	5.1 $\pm$ 0.6
	K131D <sub>7</sub> /K147D <sub>7</sub>	N/A <sup>b</sup>	2.2 $\pm$ 0.2	N/A <sup>c</sup>	2.0 $\pm$ 0.2
AK	WT- $\alpha$ HL	9.3 $\pm$ 0.9	1.3 $\pm$ 0.1	0.04 $\pm$ 0.01	1.2 $\pm$ 0.5
	K131D <sub>7</sub>	2.5 $\pm$ 0.1	0.57 $\pm$ 0.02	0.21 $\pm$ 0.01	0.34 $\pm$ 0.03
	K147D <sub>7</sub>	7.9 $\pm$ 3.9	1.3 $\pm$ 0.5	N/A <sup>c</sup>	1.3 $\pm$ 0.3
	K131D <sub>7</sub> /K147D <sub>7</sub>	N/A <sup>b</sup>	7.6 $\pm$ 2.0	N/A <sup>c</sup>	6.2 $\pm$ 2.0

<sup>a</sup> All experiments were carried out in symmetrical conditions of 1 M KCl, 10 mM potassium phosphate, pH 7.4. A 34  $\mu$ M portion of polypeptide was added to the trans chamber. The values represent means  $\pm$  SDs calculated from three separate single-channel experiments. <sup>b</sup> The short-lived voltage-independent events "1" were undetectable. <sup>c</sup> The rate constant of association was not determined, because the events exhibited a probability lower than 0.1%.

reduction of the free energy barrier, revealing the catalytic role played by the two attractive traps in polypeptide translocation through the  $\alpha$ HL pore.

**The Effect of the Hydrophobicity of the Polypeptide.** The single-channel recordings (Figure 3) revealed that the polypeptide–pore interaction is dependent not only on the binding sites, but also the nature of the polypeptide substrate. More hydrophobic peptides exhibited a lower rate constant of association ( $k_{\text{on}-2}$ ). As shown in Table 2 and Figure 3, the rate constants of association  $k_{\text{on}-2}$  span over at least 5 orders of magnitude for the three polypeptides examined in this work. This variability was strongly dependent on the hydrophobicity index of the translocating polypeptide (Table 1). Syn B2, a highly hydrophilic polypeptide, exhibited values of  $k_{\text{on}-2}$  between  $(4.4 \pm 1.3) \times 10^5$  and  $(1.2 \pm 0.1) \times 10^7 \text{ M}^{-1} \text{ s}^{-1}$  for the WT- $\alpha$ HL and K131D<sub>7</sub>/K147D<sub>7</sub> pores, respectively (Table 2). Remarkably, much lower association rate constants were observed with the hydrophobic AK polypeptide, between  $(8 \pm 2) \times 10^2$  and  $(4.1 \pm 0.7) \times 10^5 \text{ M}^{-1} \text{ s}^{-1}$ , respectively. Overall, the kinetic rate constants  $k_{\text{on}-2}$  increased from the hydrophobic to hydrophilic polypeptides.

Consistently, these results show that the energetic barrier is greater for the hydrophobic polypeptides due to the hydrophilic nature of the pore lumen. Control experiments for determining the polypeptide concentration in the bath were carried out by quantitative ninhydrin assay (data not shown).<sup>39</sup> These controls were performed to rule out that a decrease of the  $k_{\text{on}}$  rate constant is primarily caused by the partitioning of hydrophobic polypeptides into the lipid bilayer. Interestingly, these results might explain the requirement of hydrophobic binding sites within translocons<sup>4,40,41</sup> to dramatically reduce the energetic barrier for translocating hydrophobic fragments of the polypeptide substrates. Collier and co-workers found that a phenylalanine clamp ( $\phi$ -clamp) of the PA<sub>63</sub> channel of anthrax toxin functions as a catalyzing factor for the translocation of the N-terminal domains of the lethal (LF<sub>N</sub>) and edema factor (EF<sub>N</sub>).<sup>4</sup> The translocation of polypeptides is paradoxically accelerated by a less-conductive

and narrower  $\phi$ -clamp-containing PA<sub>63</sub> channel compared with a more conductive and wider  $\phi$ -clamp-lacking PA<sub>63</sub>, concluding that the  $\phi$ -clamp represents a trap that can grasp successive hydrophobic segments in LF<sub>N</sub> and EF<sub>N</sub>.<sup>40</sup> In a very recent follow-up work, Melnyk and Collier discovered that a loop network within the pore lumen is required to position the  $\phi$ -clamp of exposed Phe residues in an active conformation, revealing the complexity of the mechanisms of the protein translocation machinery.<sup>41</sup> The studies in Collier's group reinforce that further experimentation is needed for exploring the translocation through simpler  $\beta$ -barrel models to infer the basic rules that govern this ubiquitous molecular process in biology.

**Concluding Remarks and Future Prospects.** Recent work demonstrates that a robust nanopore can represent a versatile single-molecule tool for exploring protein unfolding triggered by chemical denaturants.<sup>42</sup> With a few exceptions, both the basic biophysics<sup>19,43</sup> and the potential biotechnological applications<sup>17,44,45</sup> of protein translocation still remain largely unexplored. Notably, single-molecule protein translocation studies are also expected to inspire new theoretical efforts, especially in molecular dynamics simulations attempting an atomistic description of polypeptide translocation through protein translocases.<sup>46–49</sup>

We show here an experimental strategy to illuminate various kinetic contributions to polypeptide translocation through a  $\beta$ -barrel protein pore. These contributions were identified by either engineering negatively charged binding sites within the pore lumen or alterations of the polypeptide features. Binding sites engineered within the lumen revealed major changes in the free energy barrier for polypeptides to traverse the pore and

(39) Sarin, V. K.; Kent, S. B.; Tam, J. P.; Merrifield, R. B. *Anal. Biochem.* **1981**, *117*, 147–157.

(40) von Heijne, G. *Science* **2005**, *309*, 709–710.

(41) Melnyk, R. A.; Collier, R. J. *Proc. Natl. Acad. Sci. U.S.A.* **2006**, *103*, 9802–9807.

(42) Oukhaled, G.; Mathe, J.; Biance, A.-L.; Bacri, L.; Betton, J.-M.; Lairez, D.; Pelta, J.; Auvray, L. *Phys. Rev. Lett.* **2007**, *98*, 158101.

(43) Stefureac, R.; Long, Y. T.; Kraatz, H. B.; Howard, P.; Lee, J. S. *Biochemistry* **2006**, *45*, 9172–9179.

(44) Sutherland, T. C.; Long, Y. T.; Stefureac, R. I.; Bediako-Amoa, I.; Kraatz, H. B.; Lee, J. S. *Nano. Lett.* **2005**, *4*, 1273–1277.

(45) Han, A.; Schurmann, G.; Monding, G.; Bitterli, R. A.; de Rooij, N. F.; Stauffer, U. *Appl. Phys. Lett.* **2006**, *88*.

(46) Huang, L.; Kirmizialtin, S.; Makarov, D. E. *J. Chem. Phys.* **2005**, *123*, 124903.

(47) Tian, P.; Andricioaei, I. *J. Mol. Biol.* **2005**, *350*, 1017–1034.

(48) Gumbart, J.; Schulten, K. *Biophys. J.* **2006**, *90*, 2356–2367.

(49) Goodrich, C. P.; Kirmizialtin, S.; Huyghues-Despointes, B. M.; Zhu, A. P.; Scholtz, J. M.; Makarov, D. E.; Movileanu, L. *J. Phys. Chem. B* **2007**, *111*, 3332–3335.



to escape through either the *cis* or *trans* opening of the  $\alpha$ HL pore. With this strategy, translocation can take place in the absence of ATP-driven cellular factors, but with tunable driving force and binding interactions between the polypeptide and the pore lumen. Furthermore, because of its unprecedented thermal stability,<sup>50</sup> the  $\alpha$ HL protein might also be employed as a  $\beta$ -barrel translocase model in temperature-dependence experiments of polypeptide translocation. These studies would have the potential to illuminate the precise nature of the polypeptide–pore lumen interaction by determining the entropic and enthalpic contributions to the thermodynamic and kinetic constants, revealing information about which process in polypeptide translocation is dominant.

Undoubtedly, a deep understanding of the complex protein translocases will be accomplished by expanding our capabilities to comprehend not only how individual parts of the pore lumen interact intimately with the translocating polypeptide, but also how they act synergistically to perform the function. In the future, single-molecule protein translocation studies with small protein precursors might unravel the mechanisms by which small passengers overcome a substantial energetic barrier to traverse a  $\beta$ -barrel protein translocase. There is a great deal of anticipa-

tion that with further experimentation the broader biophysical rules inferred from such studies will be directly applicable to various complex  $\beta$ -barrel protein translocases. Specifically, the outcomes of these studies will be essential for many future attempts at deciphering complex machineries (e.g., anthrax, botulinum, TOM, and TIM channels), generating more realistic models on protein translocation.<sup>41</sup>

**Acknowledgment.** We thank Sergey Bezrukov (NIH), Dmitrii Makarov (University of Texas at Austin), and Carl Goodrich (Syracuse University) for stimulating discussions. Aaron J. Wolfe thanks Stewart Loh (SUNY Upstate Medical University, Syracuse) for help during the circular dichroism measurements. The authors are grateful to an anonymous reviewer for a constructive recommendation in regard to the interpretation of the kinetic data. This work was supported by Syracuse University start-up funds and the National Science Foundation DMR-706517 (to L.M.).

**Supporting Information Available:** Detailed I/V profiles for the wild-type and engineered  $\alpha$ HL protein pores, ionic selectivity of the wild-type and engineered  $\alpha$ HL protein pores, parameters of the transient current blockades, circular dichroism measurements of the polypeptides. This material is available free of charge via the Internet at <http://pubs.acs.org>.

(50) Kang, X. F.; Gu, L. Q.; Cheley, S.; Bayley, H. *Angew. Chem., Int. Ed.* **2005**, *44*, 1495–1499.

JA0749340